View metadata, citation and similar papers at core.ac.uk

brought to you by CORE

provided by Bradford Scholars

UNIVERSITY of BRADFORD

Library

The University of Bradford Institutional Repository

http://bradscholars.brad.ac.uk

This work is made available online in accordance with publisher policies. Please refer to the repository record for this item and our Policy Document available from the repository home page for further information.

To see the final version of this work please visit the publisher's website. Access to the published online version may require a subscription.

Link to publisher version: *https://doi.org/10.1016/j.apacoust.2017.05.035*

Citation: Khan A, Mohamed M, Al Halo N et al (2017) Acoustical properties of novel sound absorbers made from recycled granulates. Applied Acoustics. 127: 80-88.

Copyright statement: © 2017 Elsevier. Reproduced in accordance with the publisher's self-archiving policy. This manuscript version is made available under the Creative Commons *CC-BY-NC-ND 4.0 license*.

Acoustical properties of novel sound absorbers made from recycled granulates

Amir Khan, Mostafa Mohamed, Naeem Al Halo, Hadj Benkreira

Abstract

This study investigates the acoustic performance of materials made using various amounts of bio-binder (cis-1, 4-polyisoprene). The filler used in making these materials was from recycled tyres which consist of nylon 6, 6 fibres bonded to rubber grains known as tyre shred residue (TSR). The materials have shown high acoustical performance especially at low binder levels, due mainly to the open porosity of the tested samples.

The paper begins with a discussion of materials made using recycled granulates. The macroscopic properties (e.g. flow resistivity, porosity, tortuosity etc.) that control the acoustical behaviour of these materials are then defined as are methods for their measurements. The acoustical characterisation of porous media is considered next, followed by discussion of the acoustic performance of the materials. The characteristics of these novel materials are illustrated through experimental and theoretical models involving sound absorption and transmission.

Introduction

Polymers, plastics and elastomers, useful as they are in the modern world, have nevertheless created an abundance of waste residues that are not normally recyclable and continue being disposed to landfills, stockpiles or illegal dumps. These are residues or scrap of materials derived from tyres, vehicles furnishing, plastic carpet tiles and the like which consist of plastic fibres trapping rubber particulates (see Figure 1). These residues are difficult to separate and then recycle, for example a single tyre granulating company can produce up to 30 tonnes of tyre shred residue per day which ends up in the landfill. This research deals with such residues and seeks to transform them into value added acoustic materials using a bio-binder (cis-1, 4-polyisoprene). The novel acoustic materials can be tailored for noise absorption or transmission loss around buildings, industrial and domestic appliances.

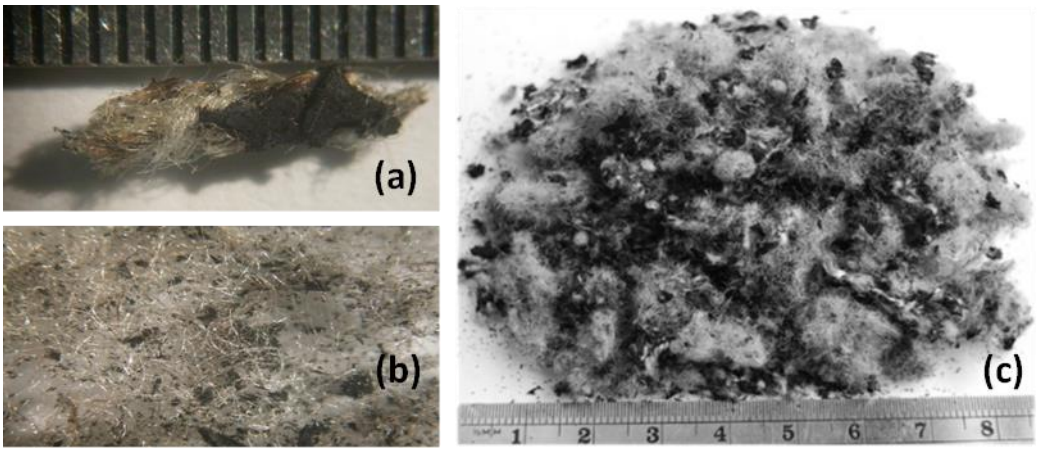

Figure 1. (a) Microscopic image of rubber crumb attached to fibres, (b) Nylon 6, 6 fibres, (c) Granulated raw tyre shred residue.

The authors are not aware of materials that have been made previously using bio-binders with tyre shred residue as the filler; the materials were produced in the acoustics laboratory at the University of Bradford. However, there has been a lot of work on the acoustical properties of sustainable materials which are made of organic waste. Works by Horoshenkov et al. [1] and Asdrubali et al. [2] have revealed the potential of sustainable materials made from recycled and natural materials. Subsequent works, some of them carried out by the present authors, have shown that natural materials could be designed to select the frequency range of maximum efficiency [3]. The aforementioned works consider that the high porosity in TSR is inherited from the fibrous component in the filler, the composition of TSR used to make the materials were 80% rubber to 20% nylon 6,6 fibres by weight. It should be underlined that some porous material manufacturing processes may give rise naturally to the existence to high porosity.

To better understand the acoustic behaviour of these materials it was necessary to characterise the materials and investigate parameters which influence the absorption mechanisms taking place within them. Furthermore, the knowledge of the internal structure of the materials would be useful to achieve a better understanding of formulating low cost materials for acoustic applications to achieve optimum sound absorption. Previous studies with a similar sustainability purpose [4] used synthetic binders to bond the particulates together to create porosity stratifications within the materials, here we use a low cost bio-binder to structure them in either partially closed or open pores.

In this paper, porous materials made using bio-binder will be characterised according to the macroscopic physical properties that determine their acoustical performance, the techniques used for measuring these quantities will be discussed. Finally, a five parameter Johnson Champoux Allard model will be used to predict the wave propagation in these materials.

Modelling Sound Propagation within Rigid Frame Porous Media

In porous media the absorption mechanisms of sound result from thermal and viscous effects occurring in the pores, in most cases the porous material is assumed to behave like a visco-thermal equivalent fluid i.e. porous material is supposed to have a rigid frame, much more rigid and heavier than air. In this situation the acoustic waves only propagate through the air within the pores of the acoustic material. In particular, viscous and inertial effects are taken into account by introducing a complex dynamic density, $\rho_e(\omega)$[kg/m^3], whereas thermal exchanges are described by a complex dynamic compressibility $K_e(\omega)$[Pa].

For the calculation of the effective properties Johnson el al (1987) proposed a semi-phenomenological model to describe the complex density of an acoustical porous material with a motionless skeleton having arbitrary pore shapes, the expressions to calculate the equivalent fluid in one pore is presented in equations 1 & 2. In the calculation of the dynamic density $\rho_e(\omega)$ four parameters are involved; the static air flow resistivity (σ), the open porosity (ϕ), the high frequency limit of the tortuosity (α_∞) and the viscous characteristic length (Λ). Champoux and Allard (1991) [5] introduced an expression (equation 2) for the dynamic bulk modulus for the same kind of porous material based on work carried out by Johnson, Koplik and Dashen [6].

$$\rho_e = \alpha_\infty \rho_0 + \frac{\sigma\phi}{i\omega}\sqrt{1+\frac{4i\,\alpha_\infty{}^2\eta\rho_0\omega}{\sigma^2\,\Lambda^2\,\phi^2}} \qquad (1)$$

and

$$K_e = \frac{k\,.\,P_0}{k-(k-1)\left[1+\frac{8\eta}{i\rho_0\,\omega\,N_p\,\Lambda'^2}\sqrt{1+\frac{i\rho_0\,\omega\,N_p\,\Lambda'^2}{16\eta}}\right]^{-1}} \qquad (2)$$

where, ρ_0 and η are the density and the viscosity of air, N_p is the Prandtl number, κ is the specific heat ratio and P_0 is the static pressure. The complex dynamic density and dynamic compressibility depend on five macroscopic parameters presented in equations 1 and 2, the airflow resistivity (σ), the open porosity (ϕ), the tortuosity (α_∞), and the viscous (Λ) and thermal (Λ') characteristic lengths.

The characteristic lengths Λ and Λ' represent the average macroscopic dimensions of the pores with respect to the viscous and thermal losses, respectively. The thermal characteristic length Λ' reflects the pores of larger size, where thermal transferring surface is significant. By contrast, the viscous characteristic length Λ reflects the importance of airflow in the pores and thus represents the smaller pores due to the high air particle velocity at these locations. In other words, Λ' stands for the average radius of the largest pores, while Λ represents the average radius of the smallest pores. The ratio Λ'/ Λ is always higher or equal to 1. Based on the work of Johnson et al. (1989), it can be shown that Λ' is generally larger than Λ if the flow is considered laminar. Further information about the above mentioned quantities can be found in [5, 6].

The characteristic impedance (Z_c) and complex wave number (k_c) can be deduced from these complex parameters, with:

$$Z_c = \sqrt{\rho_e . K_e} \quad [\mathrm{Ns/m^3}] \qquad (3)$$

and

$$k_c = \omega \sqrt{\rho_e / K_e} \quad [\mathrm{m^{-1}}] \qquad (4)$$

from which it is possible to calculate the surface impedance of a hard backed porous sample by using the following expression, were l is the thickness of the material.

$$Z_s = \frac{Zc}{\phi} . \cot (k_c l) \quad [\mathrm{Ns/m^3}] \qquad (5)$$

Experimental - Materials and sample preparation

The main raw material used was tyre shred residue from granulated tyres with fibre length ranging from 1mm to 60mm and fibre diameter in the range of 20–30μm.

The samples were prepared in a 2 litre kitchen food processor stirred by a mixer with intertwined oval wire loops into which the solid particulates and bio-binder were mixed for a time and at an impeller speed that created good distributive circulation of the solid in the mixture, Figure 2 shows a schematic of the compounding apparatus. In all formulations, it was important to first add the TSR and just enough water to ensure complete wetting of the particles on whose surface the foaming/binding was to occur. The amount of water to add to the TSR filler was determined by trial and error by determining the largest amount of water that could be added before the draining out of the mix was observed. The bio-binder was then added and mixed for a further time; the mixture was then poured into a square steel mould 20 cm x 20cm x 7cm deep. A Teflon sheet was then placed onto the foaming material and the mould closed with a lid. After a set time, the mould was opened and the final material retrieved for properties measurements. The whole procedure was carried out at room temperature of 20±5^{o}C at the extreme. The test specimens were then cut using circular cutters to 100 mm and 29 mm diameter, for testing in the impedance tube, pictures of the samples are presented in Figure 3, and Table 1 lists composition of the material mix.

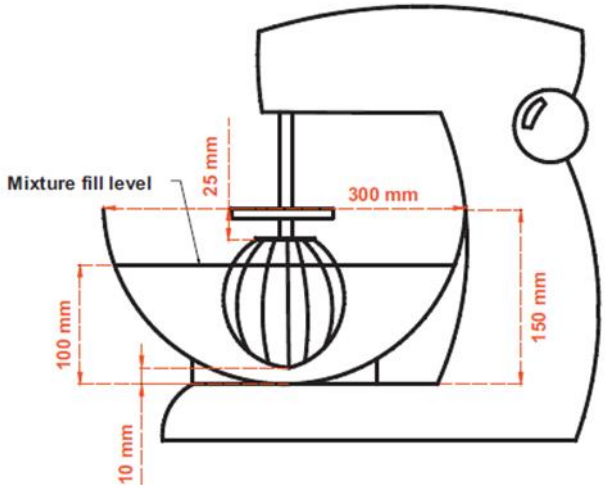

Figure 2. Schematic illustration of the compounding apparatus.

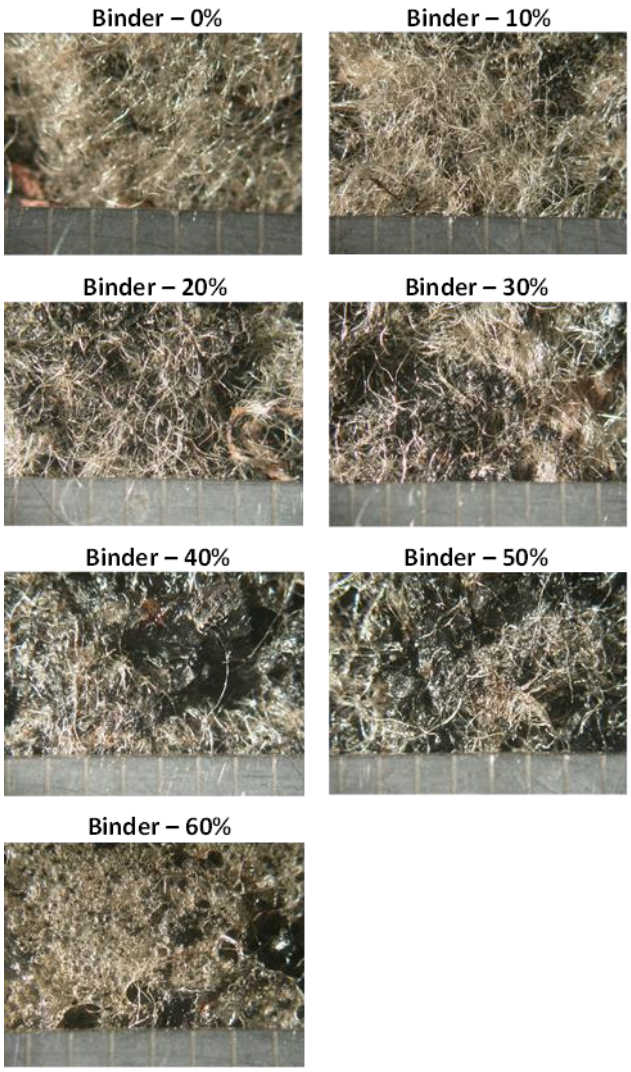

Figure 3. Microscopic photographs of samples made with various amounts of bio-binder.

Table 1. Composition of the material mix.

Binder : TSR (%)	Weight of bio-binder (g)	Weight of TSR (g)	Density (kg/m^3)
0:100	0	500	164
10:90	50	450	187
20:80	100	400	277
30:70	150	350	346
40:60	200	300	380
50:50	250	250	427
60:40	300	200	482

The bio-binder used to make the samples was supplied by Formulated Polymer Products Ltd. The experimental tests were carried out on the samples with densities between 164 and 482 kg/m^3 and a thickness of 30 mm.

The non-acoustical parameters have been experimentally determined, in particular the airflow resistivity, porosity and tortuosity. The airflow resistivity was measured according to ISO Standard 9053 [7]. Air flow resistivity or the pressure drop incurred as a result of flow through the interconnected porous structure and can help determine the extent of acoustic absorption. The air flow resistivity method used here is based on forcing a steady state or slowly oscillating air flow through a sample of the porous material. Figure 4 shows the experimental set-up used to measure the acoustic and non-acoustic properties of the materials.

The static air flow is created by releasing the air from an air cylinder (see Figure 4a). The air pressure in the compressed air line is reduced to appropriate values below 10-20 Pa through a system of adjustable valves and measured using a differential micromanometer. According to the standard procedure, the flow resistivity of a porous sample is computed by,

$$\sigma = \frac{1}{V}\frac{\Delta P}{\Delta x} \qquad (6)$$

where; V is the flow velocity (typically V < 10mm/s), ΔP is the pressure drop across the sample and Δx is the thickness of the material sample.

The open porosity was assessed using a method based on Boyle's Law as there are no agreed standard procedures for measuring the proportion of open interconnected pores (open porosity) which is required for acoustic modelling. Intuitively, one can assume that the open porosity is equal to the true porosity which can be determined from the data on the density of the material frame (ρ_f) and the density of the material itself (ρ_m). In this case the true porosity value should simply be $\phi \cong 1-\rho_m / \rho_f$. In reality, however, the true porosity value may not necessarily be equal to the proportion of open, interconnected pores which determines the actual ability of sound energy to penetrate the porous medium. A direct method for measuring the open porosity is to make use of the Boyles's law ($pV = \text{const}$, $T = \text{const}$). Recently, an improved method based on comparison of air volumes has been proposed [8]. The basic experimental setup is shown in Figure 4(b). The setup consists of two 70 ml chambers, a U-tube manometer, water drawing and air volume measurement pistons. The porosity measurement procedure starts with a calibration to equalise the volumes of the reference chamber and the measurement chamber in the absence of the sample and with the

measurement pistons set to their zero positions. The two chambers are put to atmospheric pressure by opening the valves. Valves are then closed and small amount of water is drawn. If the volumes of the two chambers are equal, then the pressure difference should be zero. Otherwise, equalising the two volumes can be achieved by adjusting the calibration piston attached to the reference chamber (see Figure 4(b)). Once the calibration has been completed, a porous sample is placed in the measurement chamber. At this stage the two chambers are opened to atmospheric pressure. The reduction in the volume of air in the measurement chamber due to the introduction of the porous solid is compensated by varying the volume of the measurement pistons. After each movement of the piston, the chambers are returned to atmospheric pressure by opening and closing the valves. As water is drawn in the successive steps, the difference in head levels between the two branches of the manometer approaches zero when the volume in the measurement pistons corresponds to the volume of solid of the porous sample. The proportion of solid (and hence the porosity) is obtained by dividing the drawn volume of air by the total volume of the sample. In the case of materials with low porosity ($\phi < 0.5$) the accuracy of this method is better than 3%. In the case of materials with medium and high porosity $\phi \geq 0.5$ the accuracy is 6-7% [9].

The tortuosity was determined using ultrasound, physically the tortuosity accounts for the twistiness of the pore in a material sample. In the simplest case this twistiness relates to the ratio of the actual path (h_e) taken by a high-frequency sound in the porous sample to the sample thickness, i.e. $\alpha_\infty \cong h_e / h$. In porous media saturated by a viscous fluid the value of tortuosity is always $\alpha_\infty > 1$ even in the case when sound propagates in the pore at normal angle of incidence. This phenomenon relates to the finite thickness of the boundary layer which is detailed in [10]. A typical setup which has been developed and used routinely at the University of Bradford for measuring the tortuosity from the ultrasonic time of flight is shown in Figure 4(c). A high-frequency tweeter is mounted at the top of a PVC tube. A 48 kHz ultrasound wave is transmitted from the tweeter and received by the two 1/4" microphones mounted on the top and on the bottom of the sample and their centres are aligned with the centres of both the sample and the tweeter. A separate measurement is carried out in the absence of the sample to determine the actual sound speed in air. The phase speed in the sample is measured by comparing the time delay (Δt) between the wave fronts of the incident and transmitted waves and making use of the expression in [10]

$\sqrt{\alpha_\infty} = \frac{c_0 \Delta t - d_m}{h}$, where $d_m = 6.35 \times 10^{-3}$ m is the diameter of the 1/4" microphone. The method is capable of measuring the tortuosity with a relatively high accuracy of 4-5%.

Finally, normal incidence sound absorption coefficient was measured according to the ISO Standard 10354-2 [11] using the Bruel and Kjear impedance tube setup shown in Figure 4(d), the physical and acoustical parameters were measured on samples of thickness 30mm.

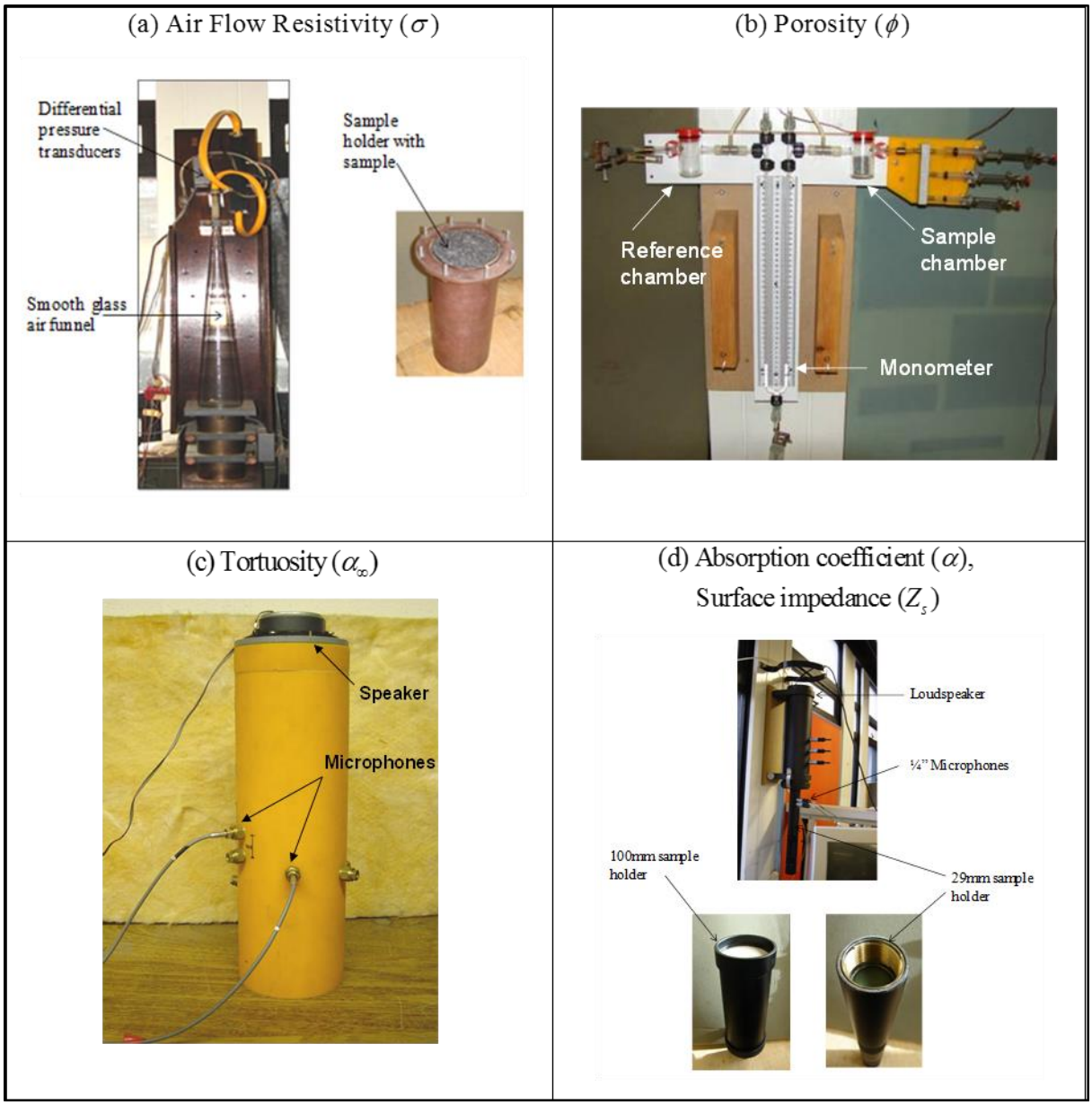

Figure 4. Experimental devices for the determination of the acoustical and physical quantities.

RESULTS

In the present study, the effects of binder to tyre shred residue ratio on the absorption coefficient performance of materials are investigated and the comparison between the samples was made over a range of audio frequencies (100-6300 Hz). The samples were tested using the small impedance tube (diameter 29mm) according to ISO 10534-2 [11], comparison was also made with a commercial product made from recycled nitrile rubber called ArmaForm Sound (AFS240) of thickness 30mm.

Complete descriptions of the tested materials are reported in Table 2. In the same table the experimental values for airflow resistivity, open porosity, tortuosity and the characteristic lengths are presented. Inverse techniques for determining the physical parameters from acoustical data have been widely investigated in recent years. Different approaches have been proposed which are based on the minimisation of the experimental characteristic or surface acoustical properties with respect to the same quantities, determined by applying a theoretical prediction model. Table 2 lists measured and predicted parameters, for inverse characterisation porosity, flow resistivity and tortuosity were all measured these measured parameters were then used to inversely derive the viscous and thermal characteristic lengths.

Table 2. The measured and deduced non-acoustical properties for the materials.

Binder : TSR (%)	σ **(exp.) (Pa.s/m^2)**	σ **(predicted) (Pa.s/m^2)**	ϕ **(exp.)**	ϕ **(predicted)**	α_∞ **(exp.)**	α_∞ **(predicted)**	**Density (Kg/m^3)**	**Thickness (m)**	Λ **(µm) (predicted)**	Λ' **(µm) (predicted)**
0:100	36,390	35,478	0.97	0.97	1.61	1.60	106	0.03	264	382
10:90	138,033	138,510	0.79	0.79	1.78	1.78	187	0.03	244	415
20:80	162,393	161,099	0.77	0.77	1.78	1.78	277	0.03	240	450
30:70	200,730	202,627	0.76	0.76	2.59	2.41	346	0.03	160	481
40:60	299,067	297,627	0.74	0.74	2.76	2.62	380	0.03	127	563
50:50	412,250	410,175	0.67	0.68	3.28	3.06	427	0.03	91	657
60:40	713,053	711,954	0.64	0.63	3.35	3.17	482	0.03	83	682

Results from Table 2 show that the variation in the airflow resistivity is between 36 and 713 kPa.s/m^2 and the values of the porosity vary between 0.64 and 0.97. Finally, the tortuosity values are between 1.61 and 3.35. The trends of various bio-binder to TSR ratios are captured in Figure 5. It is found with increasing bio-binder levels the flow resistivity, tortuosity and density increase whereas porosity decreases.

The inversely determined values for the characteristic lengths are also reported in Table 2, from Table 2 it is possible to observe that the inverse procedure provided values for the

viscous and thermal characteristic lengths between 83μm to 264μm and 382 to 682μm, respectively. In particular, it is interesting to note that viscous characteristic length which is related to the smallest pore dimensions deceases with increasing bio-binder levels and thermal characteristic length which is related to the largest pore dimensions increases with increasing bio-binder levels. By comparing the experimental physical parameters listed in Table 2 and the characteristic lengths, it is possible to underline a decrease of the airflow resistivity when the viscous characteristic length increases. Furthermore it is clear from the data that the ratio between the viscous and thermal characteristic lengths decreases with the decrease in porosity and increase in the tortuosity values, i.e. when the binder content is increased.

According to Figure 5(b) porosity decreases with increasing bio-binder levels, this is clearly reflected in the higher frequency regions in the acoustic absorption coefficient spectra (see Figure 8). For frequencies above 3 kHz there is a systematic drop in the absorption coefficient with increasing bio-binder levels. The Johnson Champoux Allard model is also able to predict the absorption coefficient with high accuracy with an error of <1%.

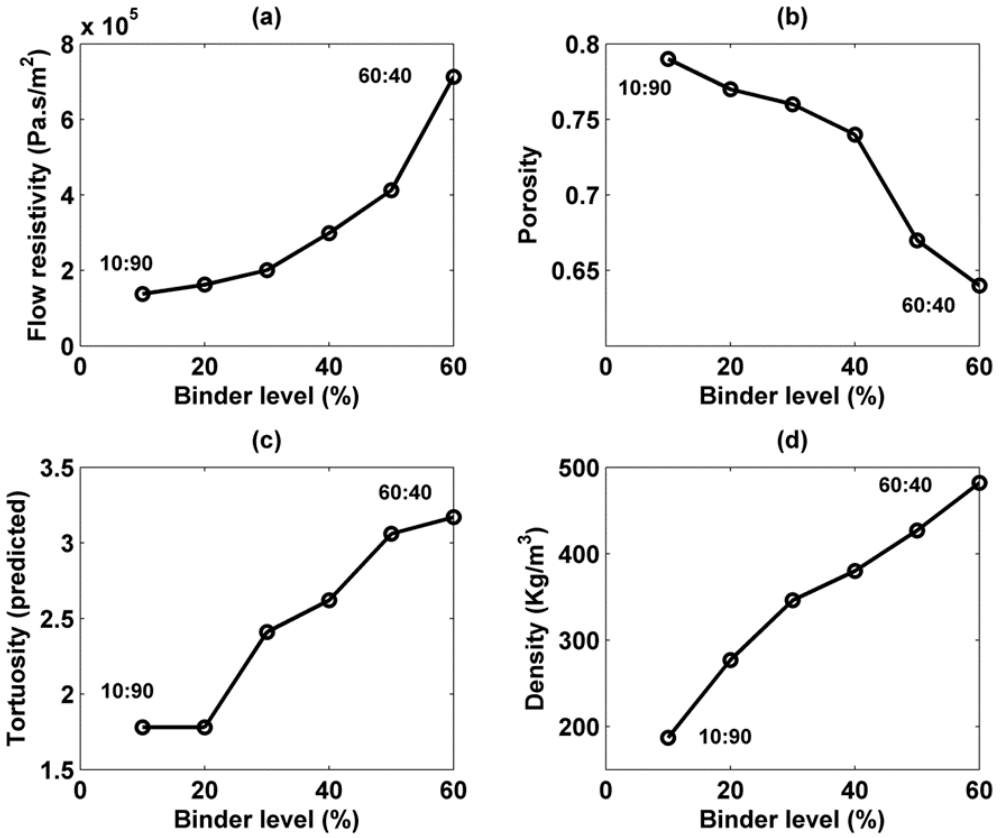

Figure 5. The dependence of the (a) flow resistivity, (b) porosity, (c) tortuosity, and (d) density on the bio-binder levels.

Three specimens were tested for acoustic absorption for each binder to TSR ratio. Figure 6 presents the measured absorption coefficient spectra for all seven materials that were prepared with different binder percentage. The grey region in the subplots shows the variability in the experimental data which was obtained for three specimens of each bio-binder to TSR ratio. The black line in these graphs corresponds to the average absorption coefficient. All samples have a low standard deviation except samples made using 20% binder levels which are showing ~20% variation in the standard deviation at around 2kHz.

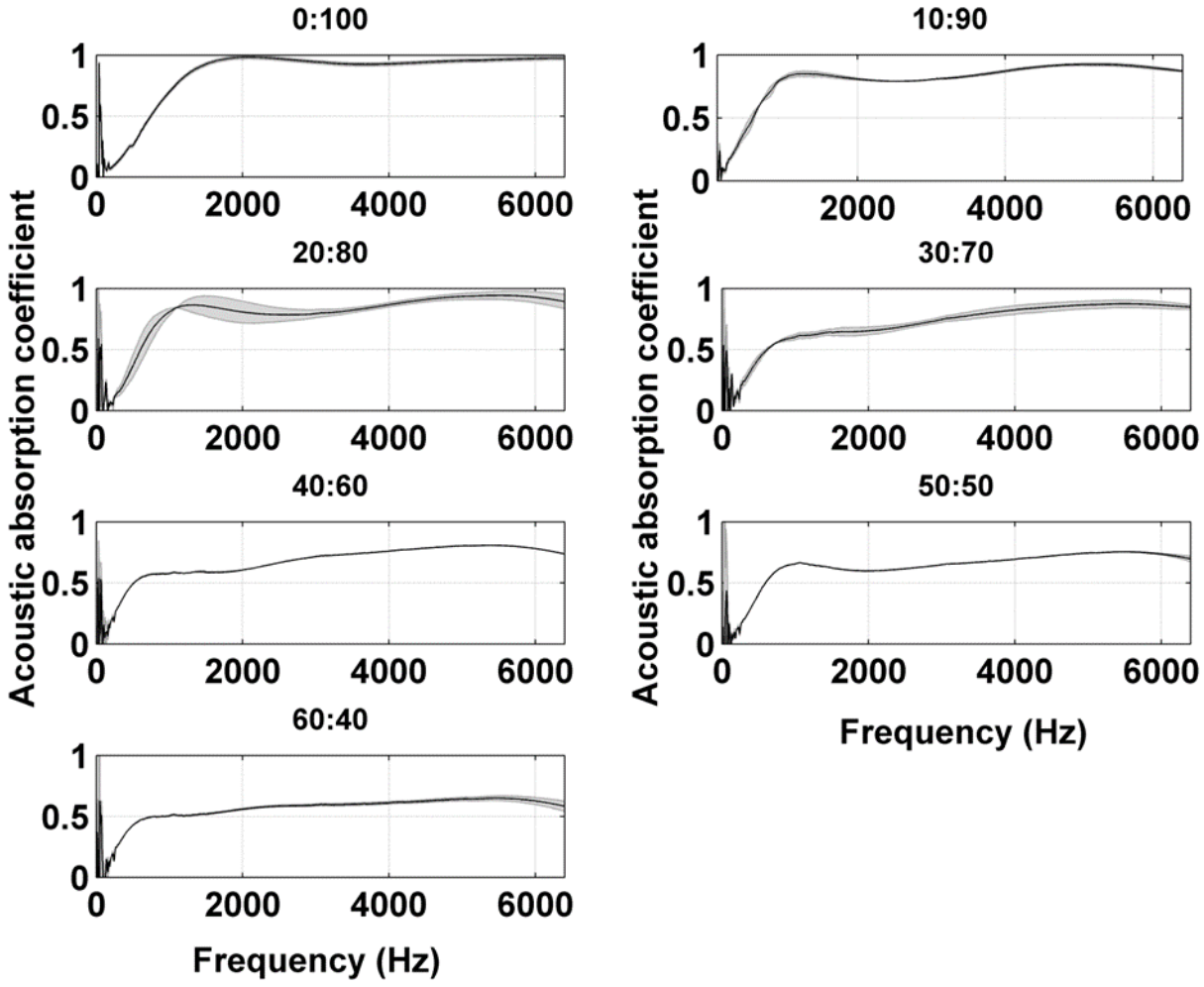

Figure 6. The acoustic absorption coefficient data for the materials (grey region shows the variation in the standard deviation for Bio-binder: TSR ratios).

Comparison between the experimental and theoretical curves of sound absorption coefficient for various bio-binder to TSR ratios are shown in Figure 7.

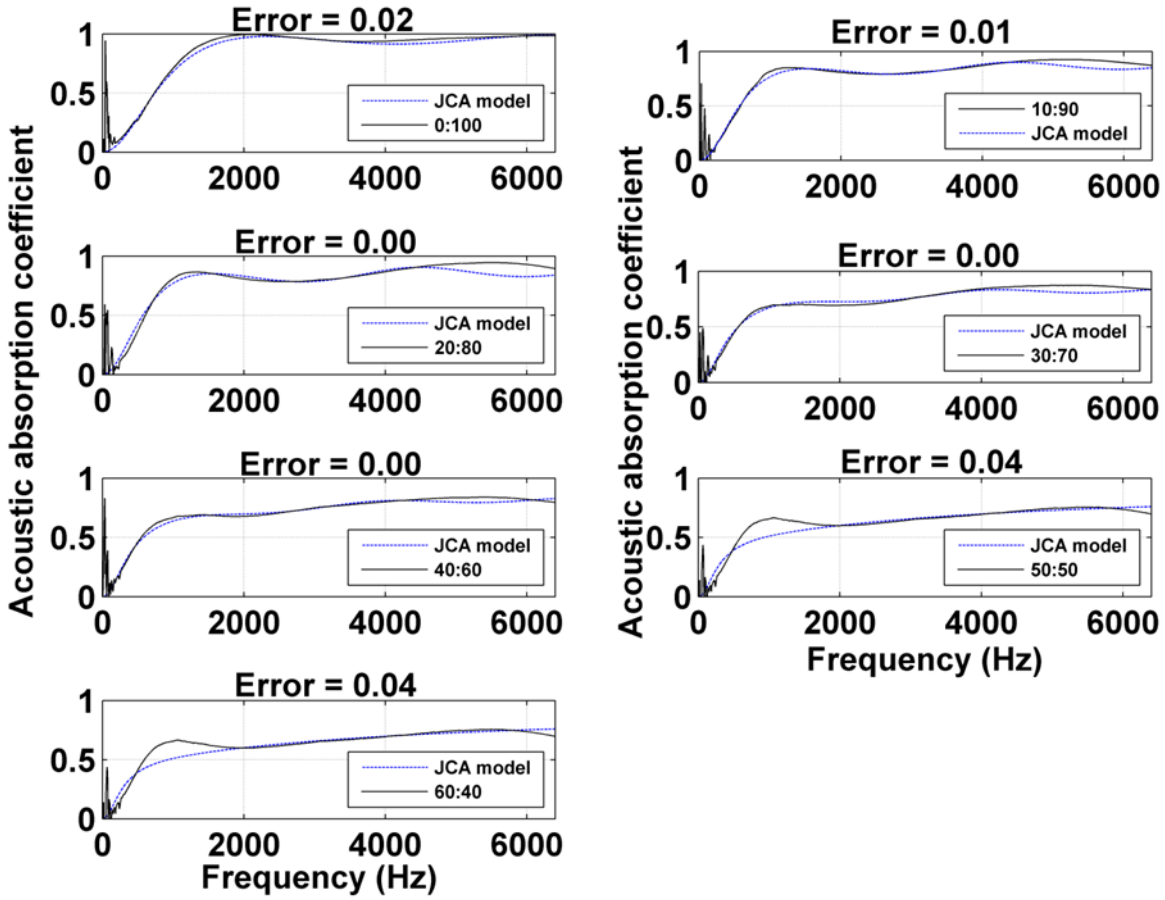

Figure 7. Measured and predicted absorption coefficient spectra for the materials using the JCA model.

A good prediction of the sound absorption is generally observed using Johnson Champoux Allard's model (1989) which is able to represent the trend of the curve over the whole frequency range. It is worth noting that there is some discrepancy for bio-binder to TSR ratios 50:50 and 60:40 for frequencies between 400Hz to 700Hz. This could be due to higher bio-binder levels creating partially closed pores. The inversely determined values of the characteristic lengths depict this behaviour for higher binder levels (see Table 2).

Furthermore it is observed that when the value of the viscous characteristic length becomes lower and airflow resistivity increases this results in higher values of sound absorption coefficient at lower frequencies i.e. material with zero percent binder level is only absorbing 0.3 whereas materials made using 10 to 60 percent binder levels are absorbing around 0.5 at

500Hz (see Figure 8). Figure 8 also presents comparison of materials made using a bio-binder with commercial material called Armaform Sound (AFS240).

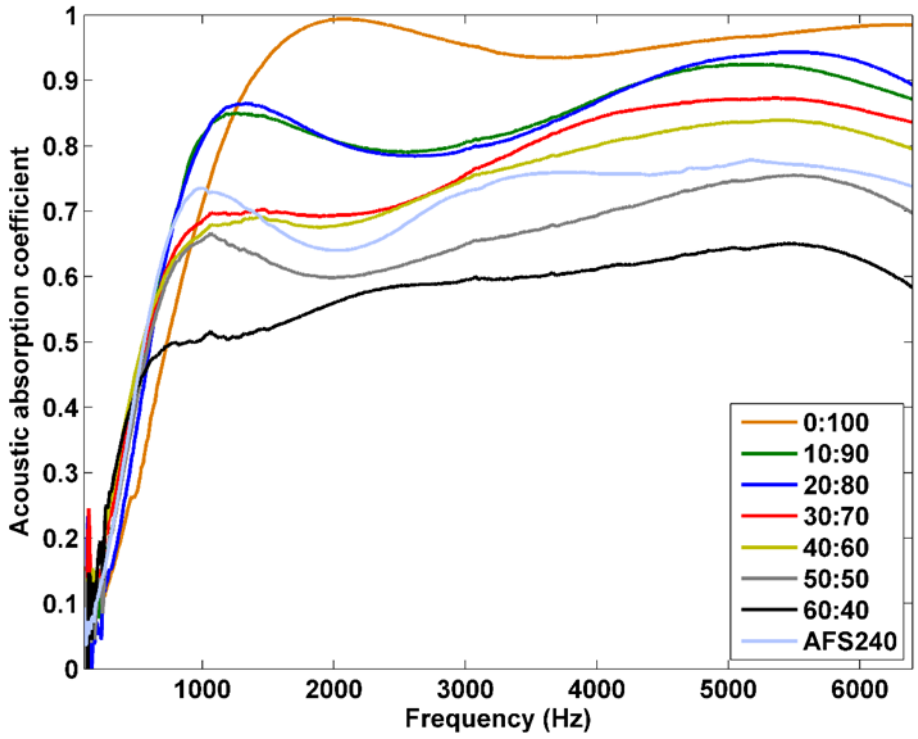

Figure 8. Measured acoustic absorption coefficient spectra for the materials.

The sound transmission loss for various binder to TSR ratios are presented in Figure 9, the transmission loss measurements were made using a 29mm Bruel & Kjear 4 microphone standing wave tube [11]. Zero percent binder level shows the lowest performance whereas sixty percent binder level shows the highest transmission loss performance. The equivalent fluid model developed by Johnson-Champoux-Allard [5, 6] was employed to make the transmission loss predictions shown in Figure 10. It is shown that the predictions based on the five parameters give similar results and are in good agreement with the transmission loss measurements. However, the resonant behaviour is not predicted due to the rigid frame assumption. Since majority of porous material frames can be approximated as acoustically rigid over a wide range of frequencies when excited by acoustic waves, the porous material can then be replaced on the macroscopic scale by an equivalent fluid of effective density $\rho_e(\omega)$ and complex dynamic compressibility $K_e(\omega)$.

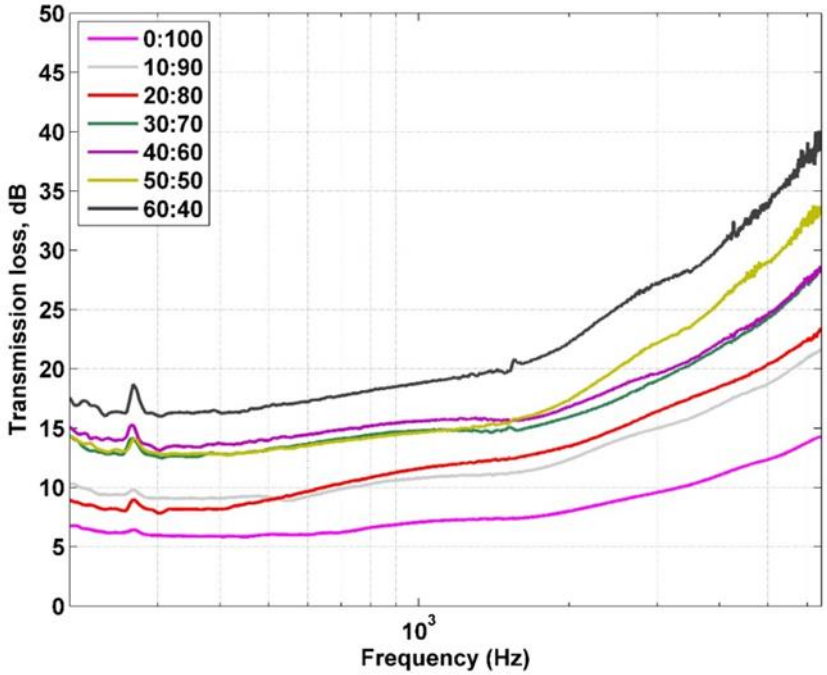

Figure 9. Comparison of the measured sound transmission loss for the materials.

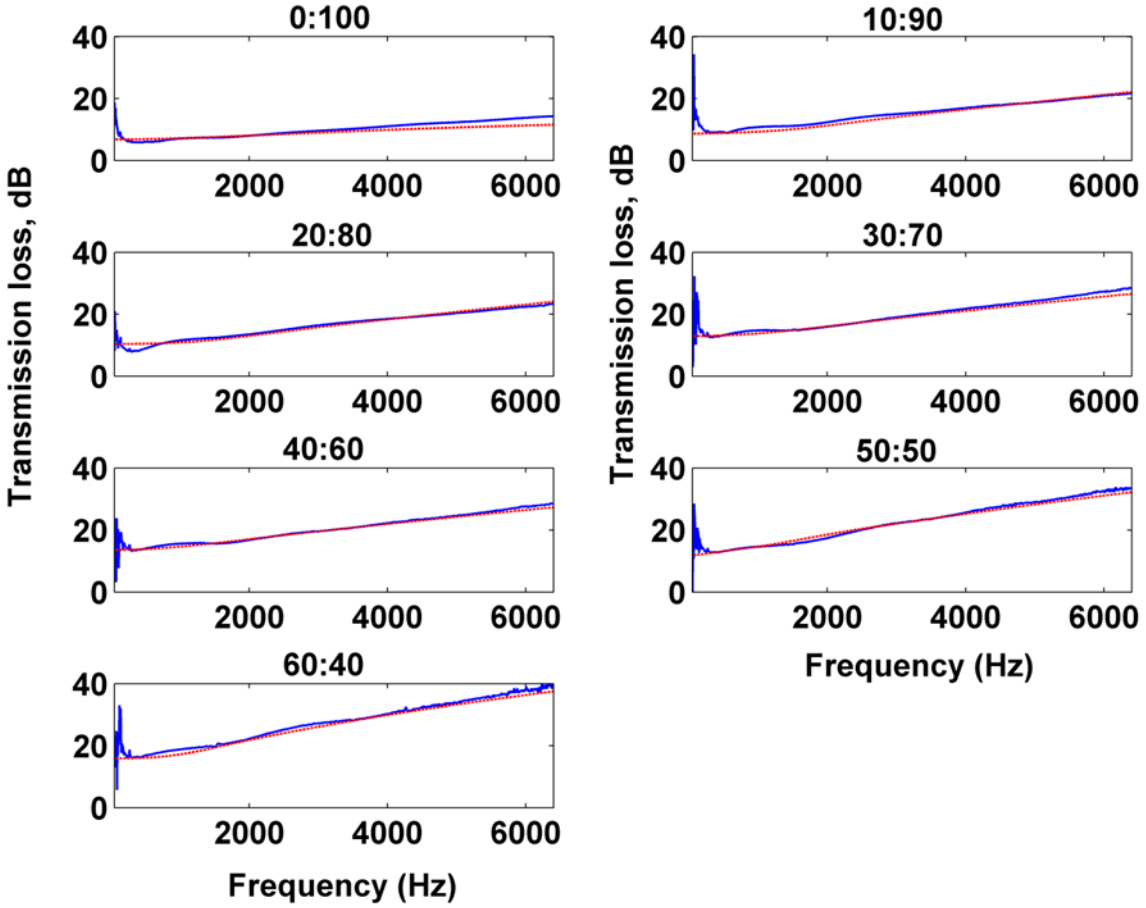

Figure 10. Comparison of sound transmission loss between measurement and predictions for various bio-binder to TSR ratios (experimental data - blue line, theoretical model – red line).

Concluding remarks

This research paper has investigated the acoustic performance of materials made using various amounts of a bio-binder (cis-1, 4-polyisoprene). The materials have shown high acoustical performance especially at low binder levels due mainly to the open porosity.

Conventional petrochemical based materials take centuries to degrade or won't degrade at all, but bio-binder polymers can decompose in a matter of months if buried in soil. This is a great advantage for materials made with bio-binders for acoustic applications. By tailoring viscoelastic and mechanical properties of bio-binder blends, it is possible to enhance acoustic and structural characteristics of materials made using bio-binders to even excel the existing petrochemical based materials. Tested materials have been experimentally characterised by measuring acoustical and non-acoustical properties. From the experimental tests carried out on the materials, they have shown high porosity at lower binder levels. In order to develop sustainable materials for acoustic applications it was necessary to focus on design of open porosity as well as modelling the link between micro structure and macroscopic properties of porous media. As a consequence a physical characterisation turned out to be necessary and some physical quantities, such as acoustic absorption coefficient, airflow resistivity, open porosity and tortuosity have been directly determined.
Furthermore, an optimisation algorithm based on inverse approach has been applied for the determination of the viscous and thermal characteristic lengths from the minimisation of the theoretical values of the acoustic absorption obtained by using Johnson-Champoux-Allard model, with respect to the values of the same quantity, experimentally measured. Results have shown a remarkable correlation between values of the airflow resistivity and viscous characteristic length. The analysis of this correlation highlights the dependence of the acoustical performance of such materials on the dimensions of the connections between the open pores. Moreover a satisfactory agreement was found between experimental data and that determined by using Johnson-Champoux-Allard model.

In conclusion, low cost sustainable materials have been produced with high acoustic performance. Furthermore the proposed investigation has shown that the combined use of experimental techniques and inversion procedures for determining physical parameters could allow to understand the internal structure of porous media and to understand their acoustical performance.

Acknowledgements

The authors would like to greatly acknowledge Kirill Horoshenkov for his comments on porous media.

REFERENCES

1. Horoshenkov K. V, and Swift M. J, " The effect of consolidation on the acoustical properties of loose rubber granulates, Applied Acoustics, 62(6), 665-690 (2001).
2. Asdrubali F, Schiavoni S and Horoshenkov K. V, "A review of sustainable materials for acoustic applications", Building Acoustics, 19(4), 283-312 (2012).
3. Khan A, Horoshenkov K. V, Benkreira H, and Mahasaranon S, "Tailoring of poro-elastic products from granular plastic and rubber waste using the cold extrusion technology, Proceedings of the Institute of Acoustic, Vol. 31 - Part 3, (2009).
4. Swift M. J, Horoshenkov K. V, "Acoustic absorption in re-cycled rubber granulates", Applied Acoustics, 57(3), 203-212 (1999).
5. Y. Champoux and J. F. Allard, "Dynamic tortuosity and bulk modulus in air saturated porous media", J. Appl. Phys. 70, 1975-1979 (1991).
6. D. L. Johnson, J. Koplik and R. Dashen, "Theory of dynamic permeability and tortuosity in fluid-saturated porous media", J. Fluid Mech. 176, 379-402 (1987).
7. ISO 9053:1991. Acoustics — Materials for acoustical applications — Determination of airflow resistance (1991).
8. P. Leclaire, O. Umnova, K. V. Horoshenkov, 'Porosity measurement by comparison of air volumes', review of scientific instruments, vol. 74, no. 3, 2003.
9. Swift, M.J. and Horoshenkov, K.V. (1999). Acoustic absorption in recycled rubber granulates. *Applied Acoustics*, **57**, 203.
10. C. Zwikker and C. W. Kosten, *Sound Absorbing Materials* Elsevier, Amsterdam, 1949.
11. EN ISO 10354-2, Acoustics-Determination of sound absorption coefficient and impedance - Part 2: Transfer-function method, 1996.

Nomenclature

$\rho_e(\omega)$	complex dynamic density
$K_e(\omega)$	dynamic compressibility
	flow resistivity
ϕ	porosity
α_∞	tortuosity
Λ	viscous characteristic length
Λ'	thermal characteristic length
ρ_0	density
η	viscosity of air
N_p	Prandtl number
κ	specific heat ratio
P_0	static pressure
Z_c	characteristic impedance
k_c	complex wave number
V	flow velocity
ΔP	pressure drop
Δx	thickness
ρ_f	density of the material frame
ρ_m	density of the material
Δt	time delay
a_{Si}	1/3 octave of sound absorption
L_i	sound pressure level